Natural Resources Canada
Ressources naturelles Canada

Preliminary mineralogy of barite-associated sulphide mineralization in the Ordovician Zn-Pb-Cu-Ag-Au Lemarchant volcanogenic massive sulphide deposit, Newfoundland and Labrador

S.B. Gill, S.J. Piercey, and C.A. Devine

Geological Survey of Canada
Current Research 2013-17

2013

Canada

Geological Survey of Canada
Current Research 2013-17

Preliminary mineralogy of barite-associated sulphide mineralization in the Ordovician Zn-Pb-Cu-Ag-Au Lemarchant volcanogenic massive sulphide deposit, Newfoundland and Labrador

S.B. Gill, S.J. Piercey, and C.A. Devine

2013

ISSN 1701-4387
Catalogue No. M44-2013/17E-PDF
ISBN 978-1-100-22488-6
doi:10.4095/292708

A copy of this publication is also available for reference in depository libraries across Canada through access to the Depository Services Program's Web site at http://dsp-psd.pwgsc.gc.ca

This publication is available for free download through GEOSCAN http://geoscan.ess.nrcan.gc.ca

Recommended citation

Gill, S.B., Piercey, S.J., and Devine, C.A., 2013. Preliminary mineralogy of barite-associated sulphide mineralization in the Ordovician Zn-Pb-Cu-Ag-Au Lemarchant volcanogenic massive sulphide deposit, Newfoundland and Labrador; Geological Survey of Canada, Current Research 2013-17, 15 p. doi: 10.4095/292708

Critical review

P. Mercier-Langevin

Authors

S.B. Gill (s.gill@mun.ca)
S.J. Piercey (spiercey@mun.ca)
Memorial University of Newfoundland
230 Elizabeth Avenue
St. John's, Newfoundland and Labrador
A1B 3X9

C.A. Devine (cdevine@canadianzinc.com)
Canadian Zinc Corporation
Suite 1710, 650 West Georgia Street
Vancouver, British Columbia
V6B 4N9

Correction date:

Preliminary mineralogy of barite-associated sulphide mineralization in the Ordovician Zn-Pb-Cu-Ag-Au Lemarchant volcanogenic massive sulphide deposit, Newfoundland and Labrador

S.B. Gill, S.J. Piercey, and C.A. Devine

Gill, S.B., Piercey, S.J., and Devine, C.A., 2013. Preliminary mineralogy of barite-associated sulphide mineralization in the Ordovician Zn-Pb-Cu-Ag-Au Lemarchant volcanogenic massive sulphide deposit, Newfoundland and Labrador; Geological Survey of Canada, Current Research 2013-17, 15 p. doi:10.4095/292708

Abstract: The bimodal felsic Zn-Pb-Cu-Ag-Au Lemarchant volcanogenic massive sulphide (VMS) deposit is located in central Newfoundland. Characteristic of the deposit is a mineralized barite lens that contains abundant sulphosalts and anomalous precious metals. While much of the barite is massive, bladed aggregates of barite are locally present. The mineralized barite lens consists of three mineral assemblages (or facies) that grade from the outer barite-rich mineralization toward the sulphide-rich base as follows: 1) facies A: white to honey-coloured sphalerite+pyrite+chalcopyrite+bornite>enargite±Au; 2) facies B: white sphalerite+galena+pyrite+tetrahedrite>tennantite+stromeyerite+Ag-tetrahedrite; and 3) facies C: honey-brown (and minor red) sphalerite+chalcopyrite+pyrite±galena. Iron content of sphalerite grades from higher values in the outer barite lens and proximal rhyolite, to lower values in the central barite lens. Minor visible free gold is present in barite-rich facies A mineralization.

The interpreted primary mineralization sequence of these three facies begins with deposition of sphalerite and fine-grained pyrite, and penecontemporaneous crystallization of tennantite-tetrahedrite, galena, and enargite, followed by sulphide replacement by bornite and chalcopyrite, late-stage stromeyerite mineralization, and recrystallization of euhedral pyrite.

The Lemarchant deposit is similar to other barite-rich, Kuroko-style VMS deposits, and is especially notable for its sulphosalt-rich mineral assemblage and precious-metal-bearing minerals. Further detailed mineral chemistry, sulphur and lead isotope analyses, and thermodynamic calculations will be undertaken to understand the siting of precious metals and the processes that resulted in precious metal enrichment at Lemarchant.

Résumé : Le gisement de Lemarchant, un gîte de sulfures massifs volcanogènes (SMV) à Zn-Pb-Cu-Ag-Au de type bimodal felsique, est situé dans le centre de Terre-Neuve. Le gisement est caractérisé par une lentille de barytine minéralisée qui contient des sulfosels en abondance et des concentrations ano males de métaux précieux. Alors que la majeure partie de la barytine est massive, des agrégats lamellaires de barytine sont présents par endroits. La lentille de barytine minéralisée est constituée de trois associations de minéraux (ou faciès) qui passent d'une minéralisation externe riche en barytine à une base riche en sulfures comme suit: 1) faciès A à sphalérite blanche à miel+pyrite+chalcopyrite+bornite>énargite±Au; 2) faciès B à sphalérite blanche+galène+pyrite+tétraédrite>tennantite+stromeyérite+tétraédrite-Ag; 3) faciès C à sphalérite miel-brune (et sphalérite rouge accessoire)+chalcopyrite+pyrite±galène. La teneur en fer de la sphalérite passe de valeurs élevées dans la lentille de barytine externe et la rhyolite proximale à des valeurs plus faibles dans le centre de la lentille de barytine. Une quantité mineure d'or natif est visible dans la minéralisation du faciès A riche en barytine.

Selon notre interprétation, la séquence primaire de minéralisation de ces trois faciès commence par le dépôt de sphalérite et de pyrite à grain fin, et la cristallisation pénécontemporaine de la tennantite-tétraédrite, de la galène et de l'énargite, suivis du remplacement des sulfures par la bornite et la chalcopyrite, de la minéralisation de la stromeyérite de phase tardive et de la recristallisation de la pyrite automorphe.

Le gisement de Lemarchant est similaire à d'autres gisements de SMV de type Kuroko riches en barytine et est particulièrement remarquable pour son association de minéraux riche en sulfosels et ses minéraux hôtes de métaux précieux. Des travaux additionnels portant sur les propriétés chimiques des minéraux, la composition isotopique du soufre et du plomb ainsi que des calculs thermodynamiques seront entrepris afin de mieux comprendre les modes de localisation des métaux précieux et les processus qui ont donné lieu à l'enrichissement en métaux précieux au gisement de Lemarchant.

INTRODUCTION

The Central Mobile Belt of Newfoundland is host to numerous past- and present-producing VMS deposits, and has been the focus of massive-sulphide exploration and development for over a century. The Lemarchant deposit, a recent discovery, is hosted within the Tally Pond volcanic belt of the Victoria Lake Supergroup (Evans and Kean, 2002; Rogers et al., 2006). This belt is also host to the currently producing Cu-Zn-rich Duck Pond deposit, and the soon-to-be-developed Boundary deposit (Squires et al., 2001; Piercey and Hinchey, 2012). The barite-rich Zn-Pb-Cu-Au-Ag-bearing Lemarchant deposit is part of the South Tally Pond property that was initially discovered by Noranda, who drilled the deposit in 1983 and from 1990 to 1993 (Squires and Moore, 2004). From 2007 to 2011, Paragon Minerals Corporation discovered the bulk of the deposit and obtained a National Instrument 43-101 resource on the deposit (Fraser et al., 2012). Canadian Zinc Corporation acquired Paragon Minerals Corporation in September 2012 and now holds a 100% interest in the property. The Lemarchant deposit has an indicated mineral resource of 1.24 Mt at 0.58% Cu, 5.38% Zn, 1.19% Pb, 1.01 g/t Au, and 59.17 g/t Ag, and an inferred resource of 1.34 Mt at 0.41% Cu, 3.70% Zn, 0.86% Pb, 1.00 g/t Au, and 50.41 g/t Ag (Fraser et al., 2012).

Despite these exploration efforts, little research has been undertaken to document the style of mineralization or to understand the high-grade base and precious-metal enrichment at the Lemarchant deposit. In particular, there has been no definition of ore facies, description of 3D ore-facies zonation, or siting of precious metals in the ore body. Initial results of field observations and preliminary petrographic and scanning-electron microscopy are presented in this report, describing the mineralization associated with barite within the Lemarchant deposit. These preliminary results are procured as part of a Masters project at the Memorial University of Newfoundland and represent a contribution to the precious-metal-rich VMS subproject of the Targeted Geoscience Initiative 4 program. The results provide a framework for further detailed work on the Lemarchant deposit, and a means of comparing Lemarchant to other Au-Ag-bearing VMS deposits in Canada and globally.

REGIONAL GEOLOGICAL SETTING

The Lemarchant deposit is hosted in Early Paleozoic accreted island-arc and rifted-arc complexes that comprise the eastern North American Appalachian Orogen (van Staal et al., 1998). The deposit is located south-southeast of the Red Indian Line, which defines a Silurian-age suture between peri-Laurentian and peri-Gondwanan rocks (Rogers et al., 2006; van Staal et al., 2007). The Red Indian Line also divides the Dunnage Zone, one of four tectonostratigraphic terranes that compose Newfoundland, into two subzones respectively called the Notre Dame and the Exploits subzones (Evans and Kean, 2002; van Staal et al., 2007). The Lemarchant deposit is in the Exploits subzone (Fig. 1), which is the eastern, peri-Gondwanan section of the Dunnage Zone, and is specifically hosted in the Victoria Lake Supergroup, a stratigraphic sequence younging upward and consisting of Cambrian to Ordovician-age primitive-arc, rifted-arc, back-arc to mature-arc volcanic sequences (Rogers et al., 2006; Zagorevski et al., 2007; Piercey and Hinchey, 2012). Easternmost and oldest of these volcanic belts is the Tally Pond group, an arc to arc-rift sequence that hosts the Lemarchant deposit, as well as the Duck Pond and Boundary VMS deposits (Evans and Kean, 2002; Rogers et al., 2006; Piercey and Hinchey, 2012).

The Tally Pond group is divided into two main formations (Rogers et al., 2006): the older and mafic dominated Lake Ambrose formation (~Lake Ambrose basalts of Dunning et al., 1991 and Evans and Kean, 2002), and the felsic-dominated Bindons Pond formation (~Boundary Brook formation of Dunning et al., 1991 and Evans and Kean, 2002). These formations have U-Pb ages ranging from approximately 514 to 509 Ma (Dunning et al., 1991; McNicoll et al., 2010), and the VMS deposits are hosted predominantly in felsic rocks of the Bindons Pond formation (Fig. 1, 2; Squires et al., 2001; Piercey and Hinchey, 2012). The Tally Pond group is intruded by the Lemarchant microgranite, which outcrops approximately 500 m northwest of the Lemarchant deposit (Fig. 2), and is interpreted to be a synvolcanic intrusion (Squires and Moore, 2004; Piercey and Hinchey, 2012). The Tally Pond group is crosscut by the middle Ordovician Harpoon Hill gabbro dikes and sills (Squires and Moore, 2004; Piercey and Hinchey, 2012).

East-northeast-striking folds and thrust faults intersect the Tally Pond volcanic belt, and the entire belt is overprinted by Silurian-Devonian-age greenschist metamorphism (Dunning et al., 1991; Evans and Kean, 2002; Rogers et al., 2006).

DEPOSIT GEOLOGY

The generally tabular Lemarchant deposit strikes north-northwest and is hosted in an upright anticline that is offset by the north-striking, west-dipping, Lemarchant thrust fault and four to five minor east-west trending normal faults (Fig. 2, 3; Fraser et al., 2012). The deposit consists of a thrust-imbricated succession of bimodal volcanic rocks, associated mineralization and hydrothermal sedimentary rocks (Fig. 3). Mineralization is situated at the contact between hanging-wall mafic volcanic flows and footwall felsic volcanic rocks (Fig. 3, 4). The overlying dark green mafic rocks predominantly consist of pillow lavas and massive flows that have vesicular and variably hyaloclastic flow tops (Fig. 5a). The underlying white to pale pink felsic rocks are composed of rhyolite flows, brecciated flow domes and associated volcaniclastic rocks (i.e. tuff and lapilli tuff after the definition by White and Houghton, 2006; Fig. 5b, c) that are variably spherulitic. These rocks are intruded by

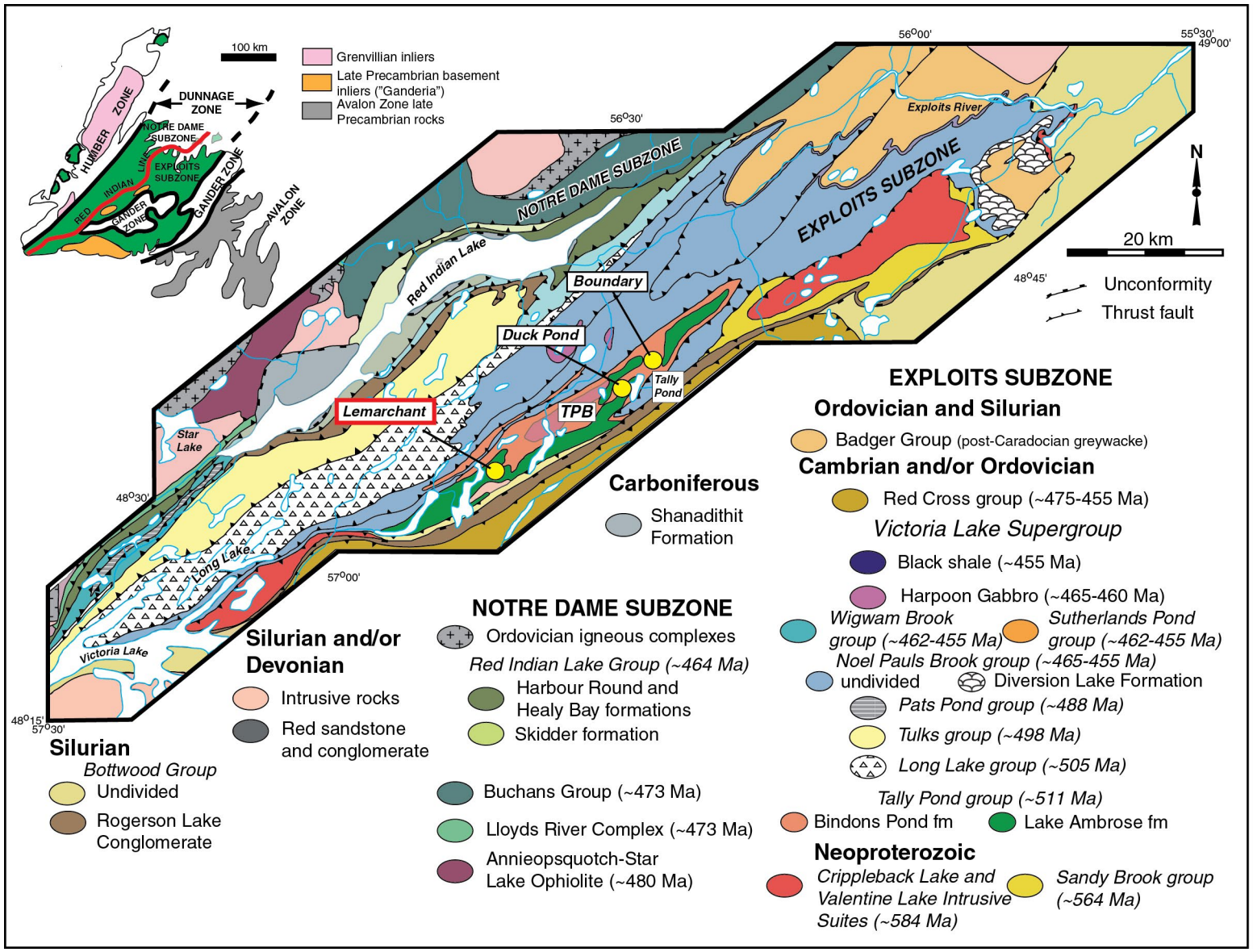

Figure 1. Geological map of volcanic belts that comprise the Exploits subzone, part of the Dunnage Zone of the Newfoundland Central Mobile Belt. The Red Indian Line suture is represented by the fault zone dividing the western edge of the Exploits subzone from the Notre Dame subzone. The Lemarchant deposit is outlined in red and shown in association with Duck Pond and Boundary deposits to the northeast. These deposits are part of the TPB (Tally Pond Belt) volcanic sequence, which lies on the eastern edge of the Exploits subzone. *Modified from* Piercey and Hinchey (2012).

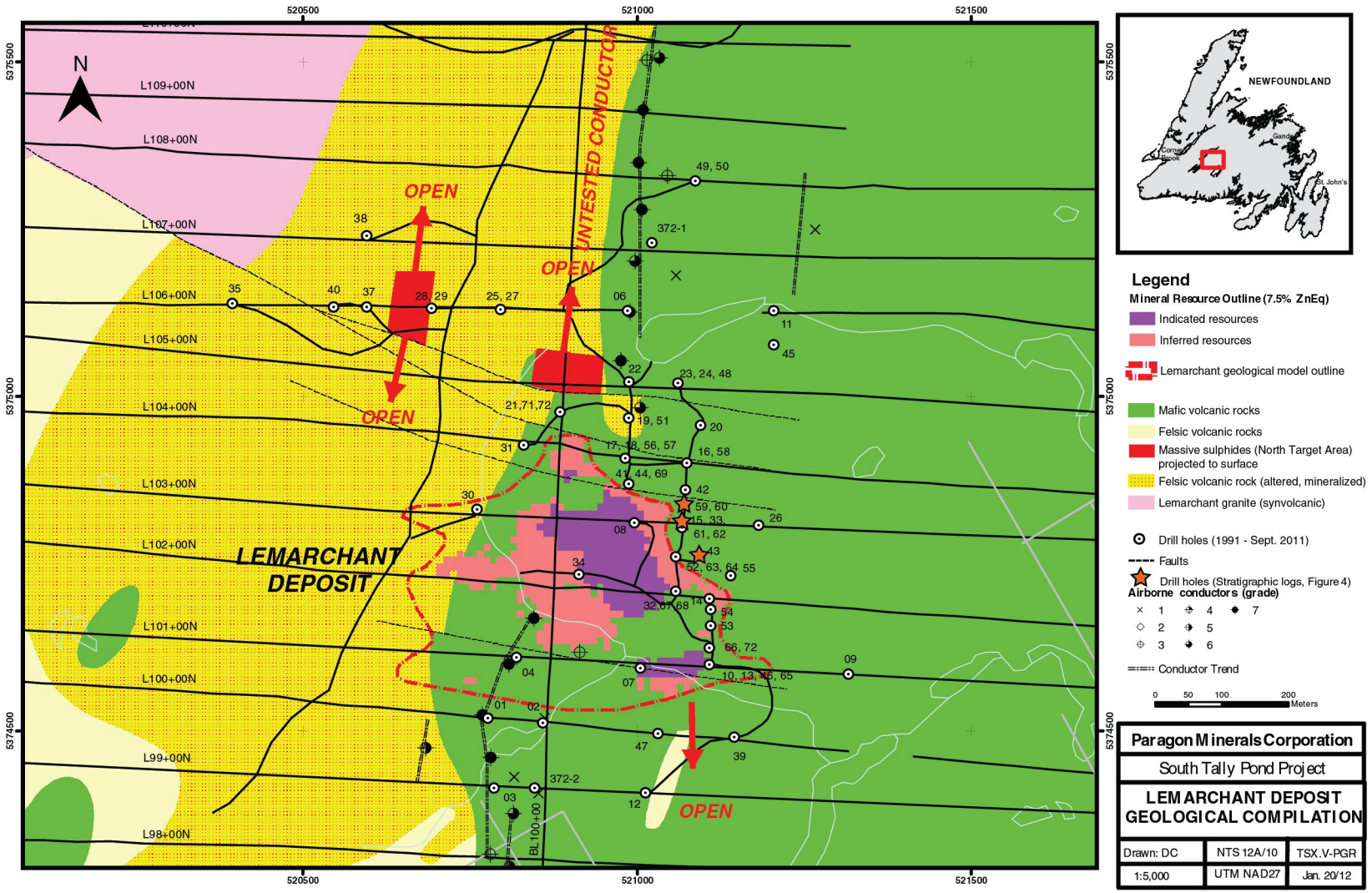

Figure 2. Map of Lemarchant geology and drill hole locations. The bimodal character of the deposit is indicated by co-dominant felsic and mafic geology, with the Lemarchant microgranite intrusion to the northwest. The pink- and purple-coloured Mineral Resource Outline represents the barite-rich mineralized zone projected to surface. A north-striking fault bisects the deposit and is crosscut by the east-west trending group of faults. Orange stars highlight drill holes represented by stratigraphic logs in Figure 4. *Modified from* Fraser et al. (2012).

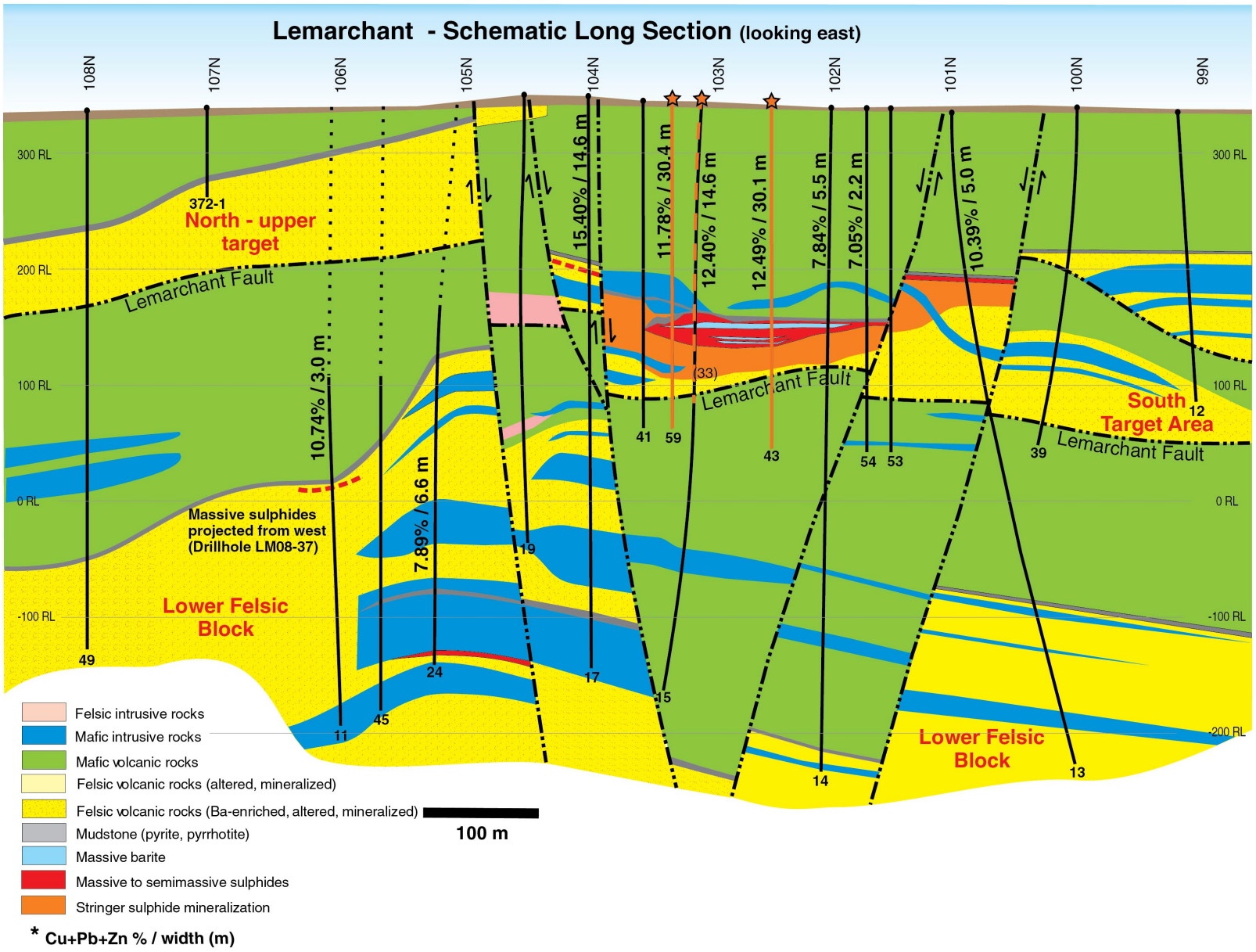

Figure 3. Long-section of Lemarchant deposit geology and drill-hole locations along section 101E. The Lemarchant fault divides the repeated sequence of bimodal mafic hanging wall rock and felsic footwall rock. Upright faults parallel each other and further offset the Lemarchant geology. The red and pale-blue lens represents massive barite and sulphide mineralized zones, which are capped by mudstones and lie at the contact between the hanging wall and footwall. Orange stars, lines and dashed lines highlight drill-hole locations and traces represented by stratigraphic logs in Figure 4. Modified from Fraser et al. (2012).

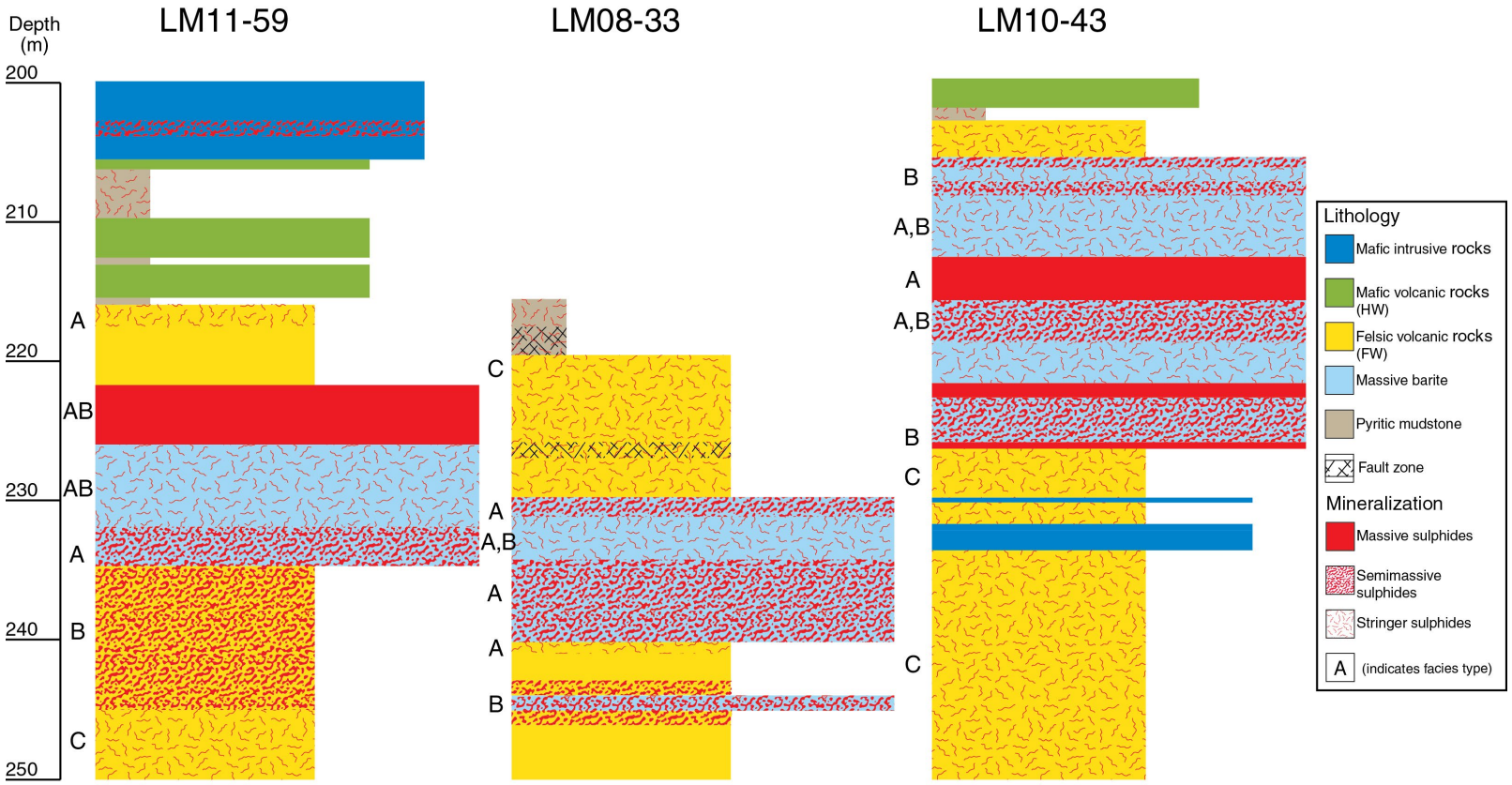

Figure 4. Representative graphic stratigraphic logs (drill holes LM11-59, LM08-33, and LM10-43) of trends in mineralization associated with the barite lens at Lemarchant (depth = 200 – 250 m). Sulphide characteristics overprint lithology as massive, semimassive and stringer mineralization; sulphide mineral assemblages/facies are indicated on the left of each column. Locations and traces of drill holes are represented by orange stars, lines, and dashed lines as in Figures 2, 3.

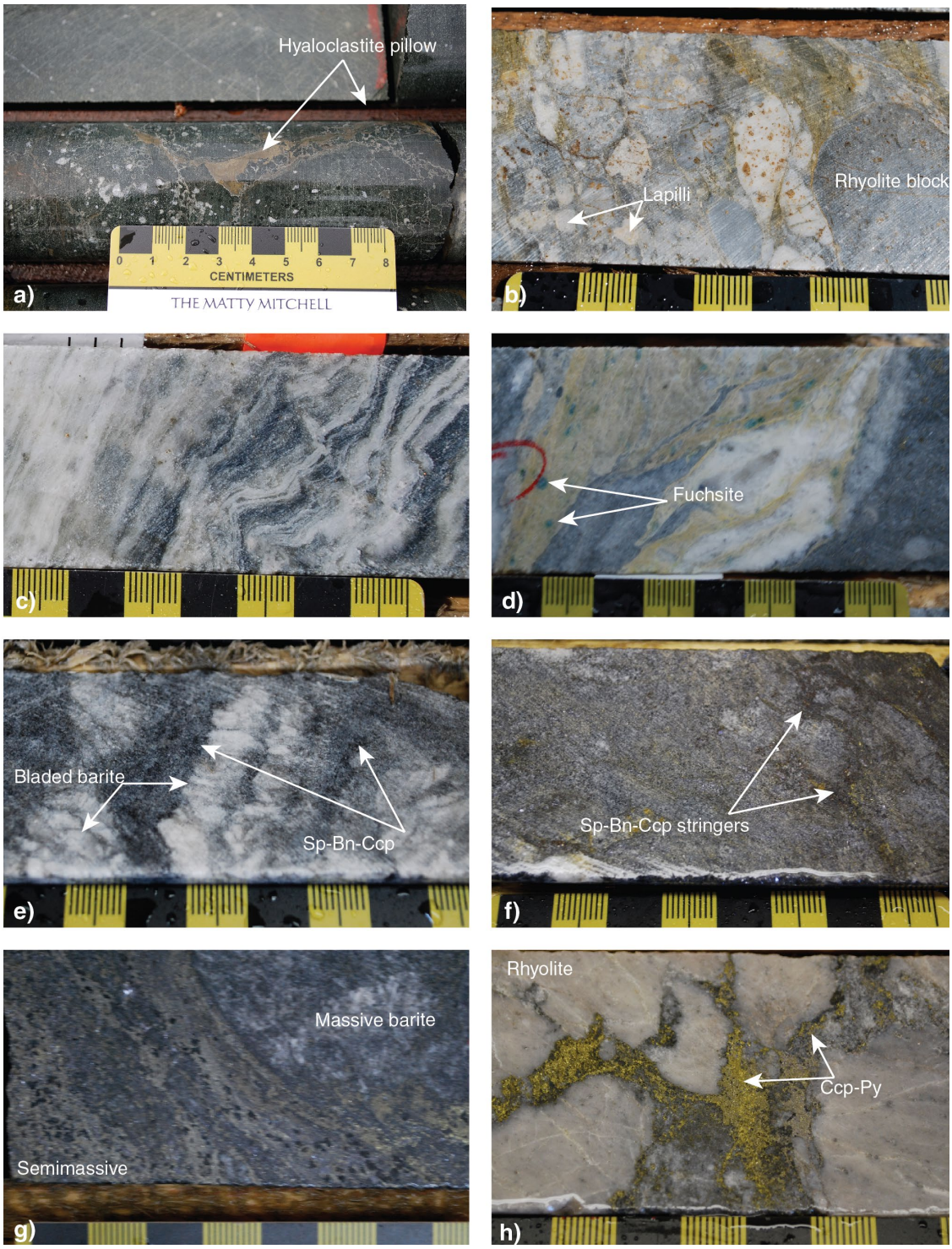

Figure 5. Drill-core photograph field mosaic of type lithologies hosting the Lemarchant deposit. Black squares = 1 cm. **a)** Mafic hanging-wall pillow lava with hyaloclastic flow-top breccia and deformed, quartz-carbonate-filled amygdules (LM07-13 at 122.80 m). 2013-215. **b)** Felsic footwall rhyolite tuff breccia, exhibiting variable alteration of lapilli and blocks (LM08-22 at 73.90 m). 2013-207. **c)** Felsic footwall flow-banded rhyolite (LM93-11 at 415.6 m). 2013-219. **d)** Wispy (synvolcanic?) fuchsite-bearing mafic dyke crosscutting footwall rhyolite tuff (LM11-70 at 94.85 m). 2013-225. **e)** Massive and bladed barite of the upper mineralized zone with crosscutting Sp-Bn-Ccp stringer sulphide mineralization (LM10-43 at 207.26 m). 2013-223. **f)** Sp-Bn-Ccp stringer and semimassive sulphide mineralization crosscutting Sp-Gn-Tnn massive sulphides (LM07-14 at 206.14 m). 2013-226. **g)** Semimassive Sp-Gn-Tnn sulphides crosscut the massive barite matrix (LM11-59 at 225.95 m). 2013-212. **h)** Ccp-Py-Sp stringer sulphide mineralization crosscutting weakly altered footwall rhyolite block breccia (LM07-14 at 207.4 m). 2013-216. Abbreviations as follows: Sp = sphalerite; Bn = bornite; Ccp = chalcopyrite; Gn = galena; Trt = tetrahedrite Tnn = tennantite; Py = pyrite. All photographs by S.B. Gill.

brown to greenish mafic dykes that are variably vesicular, fuchsite-bearing, and have irregular edges (Fig. 5d); the dykes are strongly deformed and likely synvolcanic in nature (e.g. Gibson et al., 1999). Pyritic-pyrrhotitic, sulphide-rich mudstone is found at the contact between the mineralized barite lens and the hanging wall and grades outward from the deposit; this lithostratigraphic layer is interpreted to represent a dominantly exhalative sedimentary component (Lode et al., 2012).

The Lemarchant deposit exhibits variable alteration in the footwall that grades from proximal carbonate-rich chloritic-potassic alteration to distal siliceous-sericitic alteration. The hanging wall is weakly altered, containing only minor quartz-chlorite-epidote alteration with weak silicification proximal to mineralization.

MINERALOGY AND MINERAL ASSEMBLAGES

The mineralized zones at Lemarchant lie at the contact between the mafic hanging wall and the felsic footwall. Mineralization is concentrated in a barite-rich lens that is less than 20 m thick at its centre and forms the uppermost layer in the deposit (Fig. 3). The deposit is dominated by barite in the upper and distal parts of mineralized zones, which grade downwards into sulphide-rich mineralization with barite gangue (Fig. 4). This semi-massive to massive mineralized zone extends approximately 300 m from its southern- to northernmost points (Fig. 2), and is underlain by the footwall rhyolite-hosted stringer sulphide zone (Fig. 3, 4).

The Lemarchant deposit consists of three distinct ore mineral assemblages that grade from the outer barite-dominated portion (facies A) of the deposit inward toward massive and semi-massive sulphides (facies C). Facies A consists predominantly of white to honey-coloured sphalerite+pyrite+chalcopyrite+bornite>enargite that are associated with barite and the outer portions of the mineralized zone (Fig. 4, 5e) and commonly occur as stringers crosscutting the more central facies B (Fig. 4, 5f) and facies C sulphides. Though rare, visible gold occurs in facies A stringer sulphides. The facies A assemblage grades inwards toward facies B, which consists of barite+white sphalerite+galena+pyrite+tetrahedrite>tennantite+stromeyerite (Fig. 4, 5g). Facies C rocks are mostly honey-brown sphalerite+chalcopyrite+pyrite ±galena that form the base of the barite mineralized zone, and are the dominant mineral assemblage in the footwall stringer sulphide zone underlying the barite lens (Fig. 4, 5h). Red sphalerite is rare but notable in facies C sulphides, and occurs in rhyolite proximal to outer barite mineralization (Fig. 4). The relative abundances of mineral types, including their characteristic textures or features, are summarized according to each of the described facies in Table 1.

Table 1. Modal mineralogy of sulphide facies comprising the Lemarchant VMS deposit, including significant textures and/or features of characteristic sulphide minerals. Percent values estimated from optical microscopy of polished thin sections ('Minor' implies mineral components of less than 5%).

Sulphides	Textures/features	Modal mineralogy,byfacies (% estimated)		
		FaciesA	FaciesB	FaciesC
Sphalerite	Red	0	0	10
	Honey-brown	15	0	30
	White	10	25	0
Pyrite	Fine-grained,colloform	5	0	0
	Fine-grained,euhedral	0	0	5
	Coarse-grained,rounded	10	15	10
	Coarse-grained,euhedral	0	0	10
Galena	Angular	10	20	5
	Myrmekitic	0	Minor	0
Tennantite-Tetrahedrite	Tetrahedrite(Sb-rich)	Minor	10	0
	Tennantite(As-rich)	Minor	Minor	0
	Intergrown	0	5	0
Enargite	Amorphous	5	0	0
	Myrmekitic	Minor	0	0
Bornite		5 – 15	0	0
Covellite		Minor	0	0
Chalcopyrite	Amorphous	15	10	30
	Chalcopyrite disease in sphalerite	5	5	Minor
Stromeyerite		0	5	0
Ag-rich Tetrahedrite		0	5	0

Ore Facies A

Facies A sulphides occur predominantly in barite-rich zones at the top of the deposit and interfinger with facies B (Fig. 6a-d) and C. Barite associated with mineralization is mostly massive in drill core with indistinct mineral boundaries and is variably replaced and crosscut by sulphides (Fig. 5f-g); occasionally, barite is present as elongate, bladed crystal aggregates (Fig. 5e). White or honey-coloured sphalerite is the dominant sulphide (>30% total sulphides, Table 1) and is generally semimassive and typically overgrown and crosscut by bornite, chalcopyrite, enargite, and pyrite in thin section. Occasionally sphalerite in thin section forms myrmekitic intergrowths with enargite (Fig. 6e), and atoll-type replacement in rounded pyrite. Semiquantitative SEM spectral data from massive sphalerite in the barite lens suggest it has low Fe contents (Gill, unpub. data, 2013). Pyrite occurs in two

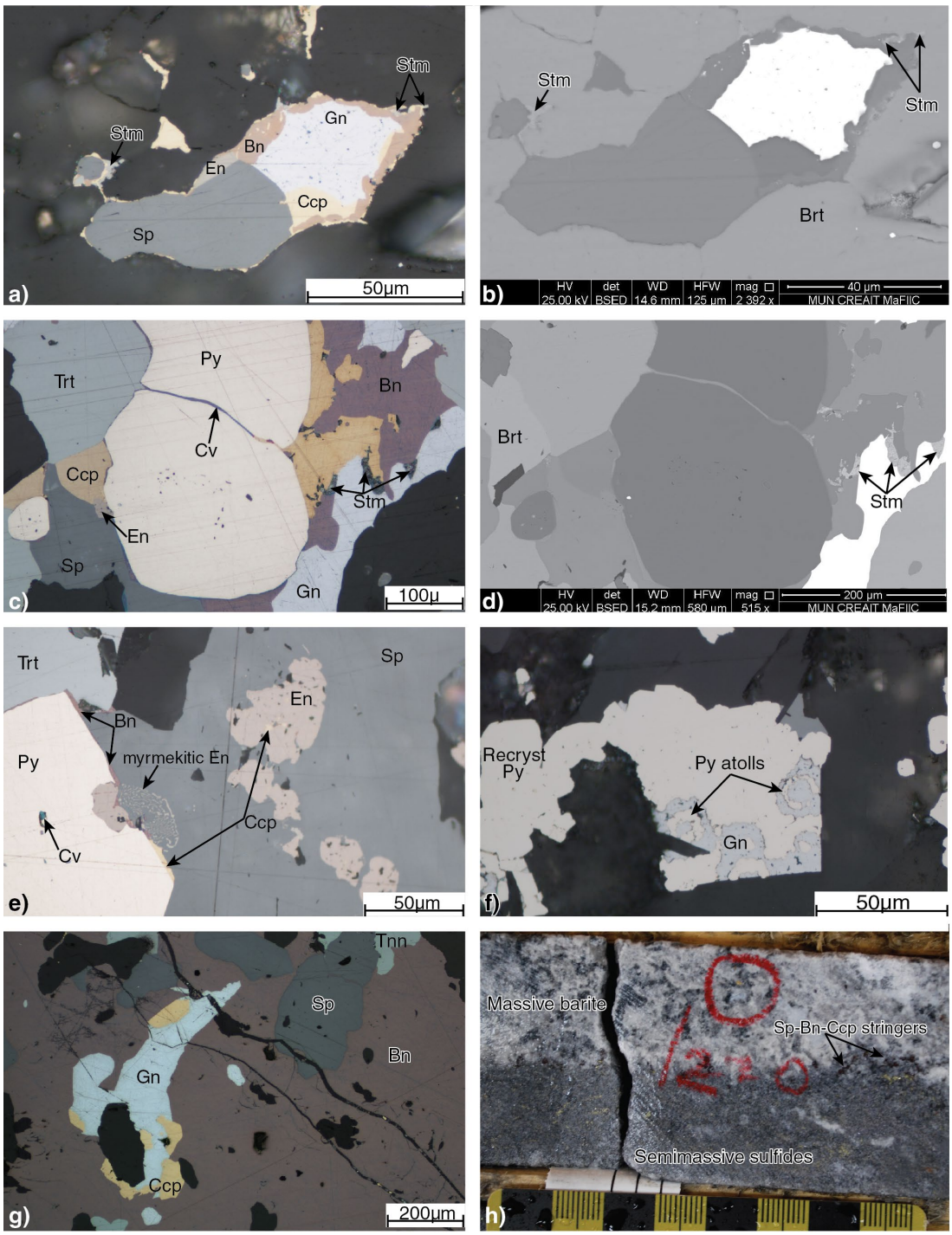

Figure 6. Thin-section photomicrographs, backscatter electron (BSE) images and drill-core photos of facies A and facies B sulfides at Lemarchant. **a)** Reflected-light photomicrograph of facies A and facies B sulphides (Bn, En, Ccp, and Stm) replacing facies B sulphides Gn and Sp at Brt-sulphide mineral boundaries (Sample CNF14259 in drill core LM07-14 at 204.44 m). 2013-213. **b)** Sample CNF14259 BSE image of Stm present at Brt-sulphide boundaries. 2013-221. **c)** Reflected-light photomicrograph of facies A sulphides (Bn, En, Ccp) overprinting facies B sulphides (Gn, Trt) and Sp in barite; Cv present at bornite boundaries is diagenetic (CNF14279 in LM08–33 at 230.75 m). 2013-230. **d)** Sample CNF14279 BSE image of irregular Stm at Ccp-Gn boundaries. 2013-227. **e)** Reflected-light photomicrograph of En myrmekitic intergrowth with Sp; Ccp and Bn present at Py, En boundaries (CNF14279 in LM08-33 at 230.75 m). 2013-211. **f)** Reflected-light photomicrograph of euhedral pyrite recrystallization from colloform Py, and relict atoll-structures formed with Gn (CNF29960 in LM11-59 at 216.00 m). 2013-220. **g)** Reflected-light photomicrograph of massive sheeted Bn in Sp, Gn and Tnn, with Ccp replacement at Gn-Bn boundaries (CNF29957 in LM11-63 at 210.83 m). 2013-209. **h)** Drill-core photo of visible gold (circled in red) in barite and associated facies A stringers (Black square = 1 cm; LM10-43 at 220.05 m). Photograph by S.B. Gill. 2013-232. Abbreviations: Bn = bornite; Ccp = chalcopyrite; En = enargite; Sp = sphalerite; Gn = galena; Stm = stromeyerite; Brt = barite; Cv = covellite; Tnn = tennantite; Py = pyrite; Trt = tetrahedrite.

distinct crystal habits in thin section: fine-grained colloform or euhedral, and coarse-grained subhedral to euhedral; however, in facies A sulphides, subhedral and corroded pyrite less than 1 mm is more abundant than fine-grained colloform pyrite. Subhedral pyrite occurs as recrystallized grains in fine-grained pyrite, and often contains galena and sphalerite inclusions in atoll-type structures (Fig. 6f). Bornite is present as medium-grained blebs in gangue and rounded pyrite, at the mineral interfaces between sphalerite, pyrite, enargite, chalcopyrite, galena, tennantite-tetrahedrite (Fig. 6a–e), and infilling fractures in gangue. Less commonly, bornite in stringers occurs as massive sheets that comprise up to 15% of the total sulphide assemblage in thin section (Fig. 6g). Covellite is occasionally present at bornite boundaries (Fig. 6c). Enargite is present as rounded to semi-angular blebs and occurs at gangue-sulphide interfaces primarily associated with sphalerite, or galena (Fig. 6a-e). Chalcopyrite is variably abundant and commonly occurs as chalcopyrite disease in sphalerite, atoll-type replacement in pyrite, and at mineral boundaries between sphalerite, pyrite, enargite, galena, tennantite-tetrahedrite, and bornite (Fig. 6a-e, g). Galena, tennantite, and tetrahedrite are not major constituents in facies A. Two occurrences of visible gold are present in facies A. Drill cores LM10–43 and LM07–14 each contain a single, approximately 1 mm gold grain that is associated with pale honey-coloured (low-Fe?) sphalerite, bornite, and chalcopyrite stringer sulphides (Fig. 6h). However, the gold in drill core LM10–43 is associated with barite-dominated facies A (Fig. 6h), whereas the gold in LM07–14 is associated with facies A stringer sulphides in the footwall rhyolite at the outer edge of the barite lens.

Ore Facies B

Facies B mineralization is massive to semimassive and lies stratigraphically below facies A mineralization (Fig. 4). These sulphides are dominated by massive white (low Fe?) sphalerite, representing less than 25% of total sulphides in thin section (Table 1). Angular galena occurs within and forms myrmekitic intergrowths with sphalerite, tetrahedrite, and tennantite, and is generally associated with sulphide-gangue boundaries (Fig. 7a-f), whereas blebby galena is present in pyrite atolls. Pyrite is present in facies B sphalerite and barite as rounded, corroded approximately 1 mm grains (Fig. 7a-d) and is variably replaced by chalcopyrite or contains galena inclusions. Tetrahedrite and tennantite are abundant in facies B (~10% total sulphides in thin section, Table 1), and, in some cases, this solid solution occurs as zoned crystals associated with galena, chalcopyrite, and barite. Semiquantitative SEM spectral data indicate tetrahedrite is As and Ag bearing (Gill, unpub. data, 2013). Angular to massive crystalline tetrahedrite has bright red internal reflections in thin section (Fig. 7b), and is more common in facies B than subangular, opaque tennantite (e.g. facies A tennantite in Fig. 6g; facies B tetrahedrite in Figures 7a-b, e-f). Stromeyerite occurs as a jagged film along chalcopyrite and galena mineral boundaries (Fig. 6c-d, 7c-d); this phase also occurs in barite with sphalerite, bornite, and tennantite-tetrahedrite (Fig. 6 a-b). Silver-rich tetrahedrite occurs in galena (Fig. 7c-d) or non-silver tetrahedrite (Fig. 7e-f), and is associated with stromeyerite and other Ag-rich sulphides (Fig. 7c-d). Silver tarnish is common to minerals in contact with stromeyerite and Ag-rich tetrahedrite (Fig. 7c, e). Chalcopyrite disease is pervasive in massive sphalerite (Fig. 7e), and commonly occurs in pyrite atolls and replaces massive galena in thin section (Fig. 6a-b, 7a); however, chalcopyrite is not a major constituent of facies B.

Ore Facies C

Facies C sulphides consist of semimassive and stringer sulphides and associated with two types of sphalerite: honey-brown sphalerite in facies C is stratigraphically lowest of the barite-rich sulphides and dominant in the footwall-hosted stringer sulphides of the stockwork zone (Fig. 4 and 5h), whereas red sphalerite in facies C is confined to the rhyolite proximal to the outer barite mineralization (Fig. 4). Honey-brown sphalerite is generally the most abundant sulphide in footwall rhyolite immediately below the barite lens (Fig. 8a) and in barite mineralization (Fig. 8b), and is associated with fine-grained pyrite and/or chalcopyrite; however, there is often a gradation into massive sheets of pyrite/chalcopyrite in thin section (Fig. 8a, c). Rarely, semimassive red sphalerite is present in the drill core in the rhyolite tuff breccia associated with the outer mineralized barite lens (Fig. 4 and 8d); semiquantitative SEM spectral analysis of red sphalerite in facies C suggests higher Fe contents than barite-hosted facies A and facies B honey- to white-coloured sphalerite (Gill, unpub. data, 2013). Sphalerite, pyrite, and galena are often replaced by blebby chalcopyrite (Fig. 8a-b), which is common to barite-rich and footwall-hosted facies C mineralization. Euhedral and subhedral pyrite can be fine grained and disseminated, or occur as coarse-grained clusters in sphalerite, chalcopyrite, and gangue; however, subhedral pyrite is more common and occurs as coarse-grained clusters of corroded, atoll-type pyrite with galena or sphalerite inclusions (Fig 8d). Pyrite in facies C stringers is increasingly euhedral with increasing depth below the barite lens (e.g. Fig. 4 and 8a). Galena is more abundant in red sphalerite (high Fe?) facies C sulphides in rhyolite associated with outer barite mineralization (Fig. 8d); sometimes anhedral or interstitial galena is present in the lower barite lens (Fig. 8b, c) and the footwall rhyolite immediately underlying barite mineralization (Fig. 8a).

SUMMARY

The Lemarchant VMS deposit is hosted in a bimodal-felsic lithostratigraphic sequence and has Au-Ag-bearing, Kuroko-style Zn-Pb-Ba mineralization. Sulphide mineralization can be divided into three general assemblages or facies (*see* Table 1): A) semi-massive to stringer white- to honey-coloured sphalerite+pyrite+chalcopyrite+bornite>

enargite±galena+tennantite-tetrahedrite; B) massive and semi-massive white sphalerite+galena+pyrite+tetrahedrite> tennantite+stromeyerite+Ag-rich tetrahedrite+chalcopyrite; and C) semi-massive to stringer honey-brown or red sphal erite+chalcopyrite+pyrite±galena. Visible gold is only associated with facies A, and no microscopic gold occurrences (i.e. native gold, electrum) have yet been noted; however, the similarities between SEM back-scatter-electron characteristics of barite, galena, tetrahedrite, Ag-rich tetrahedrite, and gold requires more detailed SEM-mineral liberation analysis (SEM-MLA) to distinguish such fine-grained gold. Iron contents of sphalerite associated with barite appear to be generally low as deduced from semiquantitative SEM spectra and colour variations in drill core and thin section. This is consistent with the correlation made by Hannington and Scott (1989) regarding gold enrichment in VMS deposits characterized by Fe-poor sphalerite; however, Fe concentration does grade from slightly higher values at the outer fringes of barite in the deposit (i.e. facies A), with which free gold is associated, toward lower values at the centre of the barite lens (i.e. facies B; Gill, unpub. data, 2013).

Characteristic textures and mineral associations of sulphides comprising the Lemarchant deposit suggest facies B deposition preceded that of facies A and facies C, and

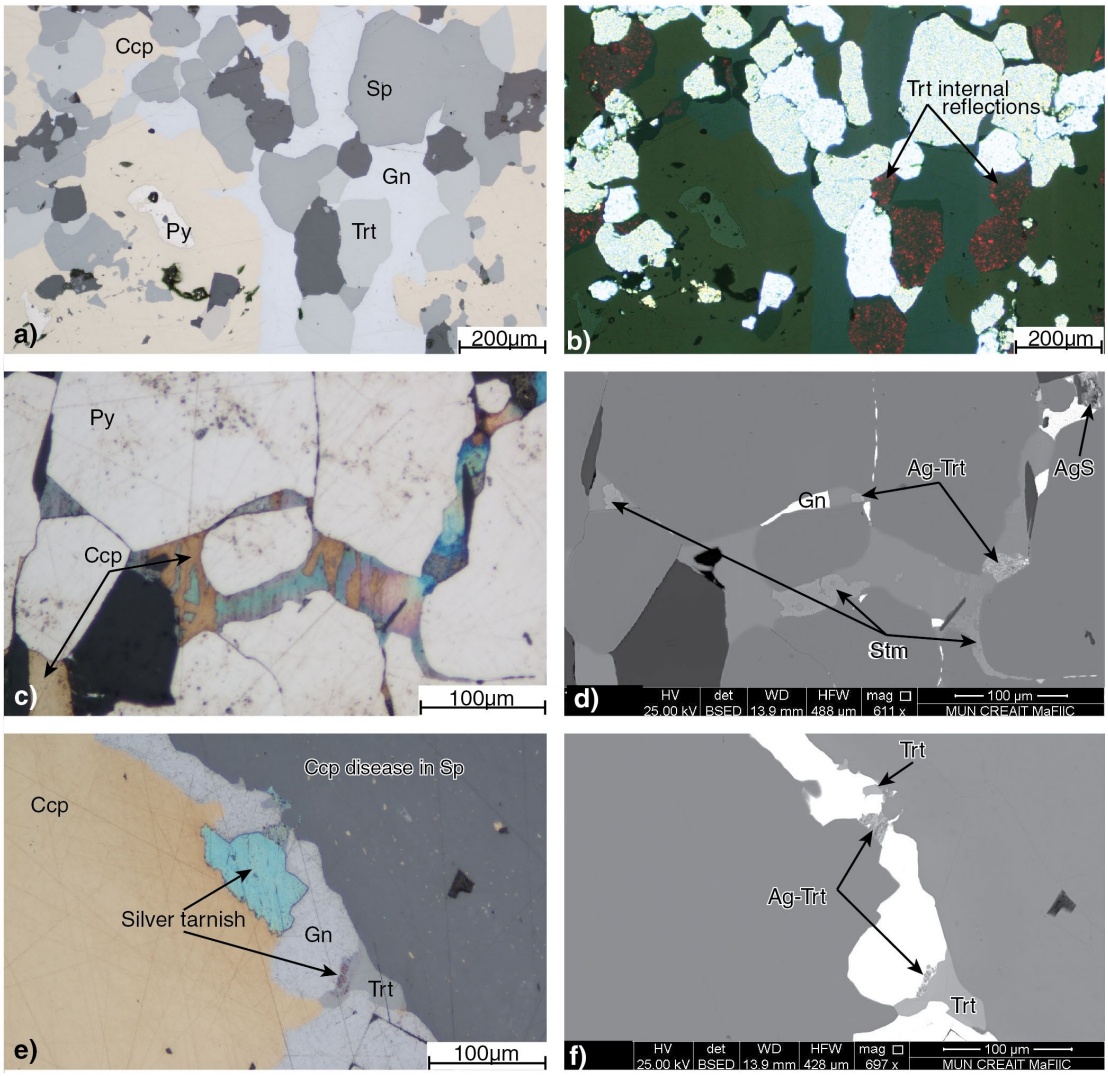

Figure 7. Thin-section photomicrographs and BSE images of facies B sulfides at Lemarchant. **a)** Reflected-light photomicrograph of Ccp replacement of angular Trt, sheeted Gn and rounded Py (Sample CNF29957 in drill core LM11-63 at 210.83 m). 2013-224. **b)** Transmitted-light photomicrograph of CNF29957 showing the characteristic bright red internal reflections of Trt in facies B sulphides. 2013-228. **c)** Reflected-light photomicrograph of silver tarnish of interstitial Ccp in subhedral Py (CNF29986 in LM08-19 at 97.63 m). 2013-229. **d)** Sample CNF29986 BSE image of Stm associated with Ccp, and Ag-bearing Trt (Ag-Trt) and other silver sulphides (AgS) associated with Gn; subhedral Py with entrained Gn. 2013-214. **e)** Reflected-light photomicrograph of Sp with Ccp disease and Ccp replacement of Gn and Trt, with silver tarnish at Ccp-Gn-Trt boundaries (CNF29986 in LM08-19 at 97.63 m). 2013-231. **f)** Sample CNF29986 BSE image of Ag-bearing Trt (Ag-Trt) at Gn-Trt boundaries. 2013-210. Abbreviations: Ccp = chalcopyrite; Py = pyrite; Sp = sphalerite; Gn = galena; Stm = stromeyerite; Trt = tetrahedrite.

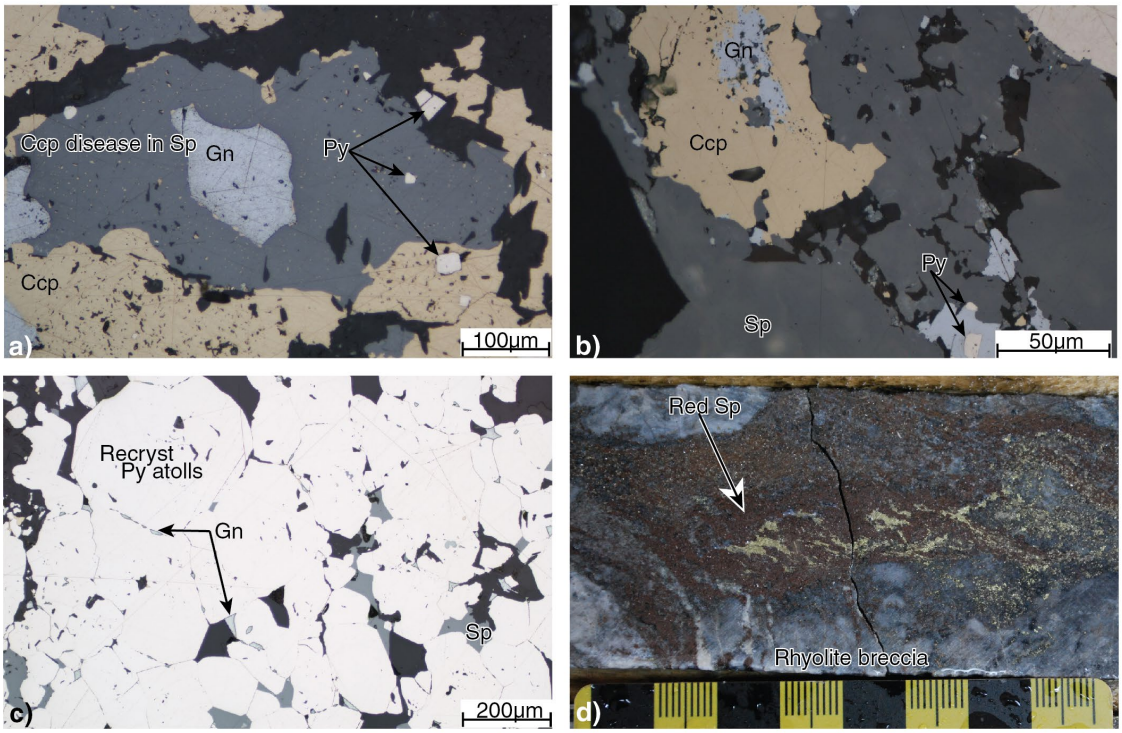

Figure 8. Thin-section photomicrographs and drill-core photos of facies C sulphides at Lemarchant. **a)** Reflected-light photomicrograph of massive Sp with Ccp disease and Ccp replacement at Sp-gangue and Sp-angular Gn boundaries; euhedral Py overprinting Sp, Ccp, and gangue (Sample CNF14288 in drill core LM11-68 at 235.10 m). 2013-217. **b)** Reflected-light photomicrograph of Ccp replacement of Gn in Sp; subhedral to euhedral Py in Gn, Sp, and gangue (CNF29965 in LM07-15 at 233.20 m). 2013-208. **c)** Reflected-light photomicrograph of recrystallized subhedral Py with entrained Gn in relict atoll-structures (CNF29985 in LM08-19 at 96.25 m). 2013-222. **d)** Drill-core photo of red Sp-Ccp-Py stringers crosscutting footwall rhyolite tuff breccia (Black square = 1 cm; LM08-33 at 219.83 m). Photograph by S.B. Gill. 2013-218. Abbreviations: Ccp = chalcopyrite; Sp = sphalerite; Gn = galena; Py = pyrite.

indicate that silver enrichment occurred late in the mineralization sequence. The paragenesis of sulphide-mineral phases encompassing all facies can be described as follows (Fig. 9): 1) initial crystallization of fine-grained pyrite and sphalerite was coincident with tennantite-tetrahedrite (±Ag-rich tetrahedrite), galena, and enargite deposition; and 2) later replacement of sulphides by chalcopyrite and bornite (accompanied by gold precipitation?) that overlapped with late-stage stromeyerite deposition and mid- to late-stage recrystallization and coarsening to euhedral pyrite. Primary mineralization may be partially obscured by later remobilization of more tractable sulphide phases (e.g. bornite in fractured gangue) during metamorphism and deformation and requires further investigation.

The depositional sequence of mineralization and the composition of sulphides and sulphosalts at Lemarchant (e.g. tennantite-tetrahedrite and enargite followed by bornite and chalcopyrite) suggest that hydrothermal fluid temperatures were initially low to moderate (<250°C), and later rose to slightly elevated temperatures associated with recrystallization of fine-grained pyrite to euhedral pyrite (Eldridge et al., 1983; Hannington and Scott, 1989; Roth et al., 1999). Furthermore, the mineral assemblages of the Lemarchant deposit that include abundant sulphosalts and high-sulphidation mineral assemblages (e.g. enargite-tennantite-tetrahedrite), anomalous Au-Ag phases, and locally bladed barite, are features atypical of normal VMS, but common to Kuroko-type VMS deposits (Shimazaki, 1974) and hybrid VMS-epithermal deposits (e.g. high-sulphidation VMS; Sillitoe et al., 1996; Hannington et al., 1999; de Ronde et al., 2005; Dubé et al., 2007; de Ronde et al., 2011).

Further research will involve additional field and microscopic documentation of sulphide minerals and sulphide-mineral facies; detailed SEM-MLA to investigate the location of fine-grained gold in thin section; electron-microprobe analyses to study compositional variations of sulphide facies; laser ablation ICP-MS for trace-element content of sulphide phases; and secondary ion mass spectrometry (SIMS) for in situ sulphur and lead isotopes. These data will help refine mineral relationships within the Lemarchant deposit, gold-silver associations, and the physiochemical conditions of deposit formation.

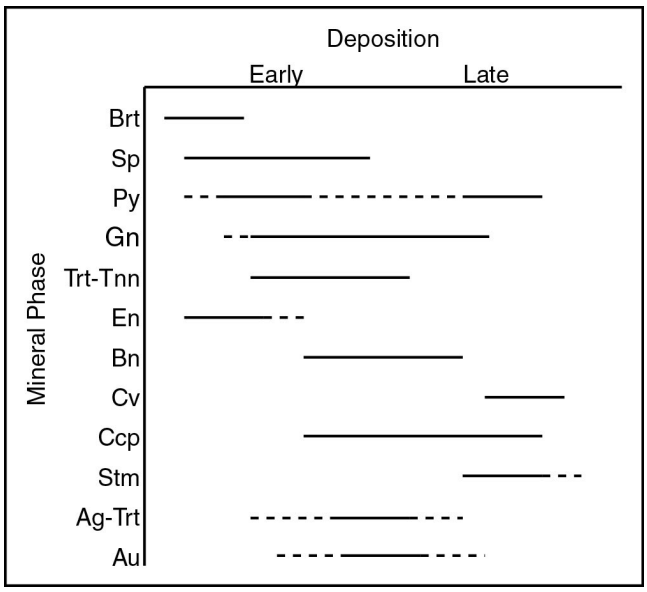

Figure 9. Diagram of interpreted, but preliminary, sulphide mineral paragenesis at Lemarchant. Relative timing of mineral deposition is indicated (solid lines) or inferred (dashed lines) by reported mineral association and textures. Mineral abbreviations as in Figures 5 to 8.

ACKNOWLEDGMENTS

This project is supported by the Geological Survey of Canada TGI-4 Grant Program. This research is also supported by additional grants to Steve Piercey, including an NSERC Discovery Grant and the NSERC-Altius Industrial Research Chair in Mineral Deposits supported by NSERC, Altius Resources Inc., and the Research and Development Corporation of Newfoundland and Labrador. Many thanks to Canadian Zinc Corporation and Paragon Mineral Corporation (a 100% owned subsidiary of Canadian Zinc) for access to the drill core and use of the Buchans Junction core shed; to Stefanie Lode (Ph.D. Candidate, Memorial University of Newfoundland) for the introduction to Lemarchant geology and insightful discussions; to Michael Schaffer for explaining the nuances of SEM analysis; and to Graham Layne for guidance in petrographic interpretation. Reviews by Patrick Mercier-Langevin and Michael Vande Guchte greatly improved this manuscript.

REFERENCES

de Ronde, C.E.J., Hannington, M.D., Stoffers, P., Wright, I.C., Ditchburn, R.G., Reyes, A.G., Baker, E.T., Massoth, G.J., Lupton, J.E., Walker, S.L., Greene, R.R., Soong, C.W.R., Ishibashi, J., Lebon, G.T., Bray, C.J., and Resing, J.A., 2005. Evolution of a submarine magmatic-hydrothermal system: Brothers Volcano, southern Kermadec Arc, New Zealand; Economic Geology and the Bulletin of the Society of Economic Geologists, v. 100, p. 1097–1133. doi:10.2113/gsecongeo.100.6.1097

de Ronde, C., Massoth, G., Butterfield, D., Christenson, B., Ishibashi, J., Ditchburn, R., Hannington, M., Brathwaite, R., Lupton, J., Kamenetsky, V., Graham, I., Zellmer, G., Dziak, R., Embley, R., Dekov, V., Munnik, F., Lahr, J., Evans, L., and Takai, K., 2011. Submarine hydrothermal activity and gold-rich mineralization at Brothers Volcano, Kermadec Arc, New Zealand; Mineralium Deposita, v. 46, p. 541–584. doi:10.1007/s00126-011-0345-8

Dubé, B., Gosselin, P., Mercier-Langevin, P., Hannington, M., and Galley, A., 2007. Gold-rich volcanogenic massive sulphide deposits; *in* Mineral Deposits of Canada: A Synthesis of Major Deposit-types, District Metallogeny, the Evolution of Geological Provinces, and Exploration Methods, Special Publication 5, (ed.) W.D. Goodfellow; Mineral Deposits Division, Geological Association of Canada; p. 75–94.

Dunning, G.R., Swinden, H.S., Kean, B.F., Evans, D.T.W., and Jenner, G.A., 1991. A Cambrian island arc in Iapetus; geochronology and geochemistry of the Lake Ambrose volcanic belt, Newfoundland Appalachians; Geological Magazine, v. 128, p. 1–17. doi:10.1017/S0016756800018008

Eldridge, C.S., Barton, P.B., Jr., and Ohmoto, H., 1983. Mineral textures and their bearing on formation of the kuroko orebodies; Economic Geology Monographs, v. 5, p. 241–281.

Evans, D.T.W. and Kean, B.F., 2002. The Victoria Lake Supergroup, central Newfoundland - its definition, setting and volcanogenic massive sulphide mineralization, Newfoundland and Labroador Department of Mines and Energy, Geological Survey; Open File NFLD, v. 2790, p. 68.

Fraser, D., Giroux, G.H., Copeland, D.A., and Devine, C.A., 2012. Technical Report and Resource Minerals Estimate on the Lemarchant Deposit, South Tally Pond VMS Project, Central Newfoundland, Canada – NI 43–101 Technical Report prepared for Paragon Minerals Corporation, 132 p.

Gibson, H., Morton, R., and Hudak, G., 1999. Submarine volcanic processes, deposits, and environments favorable for the location of volcanic-associated massive sulfide deposits; Reviews in Economic Geology, v. 8, p. 13–51.

Hannington, M. and Scott, S.D., 1989. Sulfidation equilibria as guides to gold mineralization in volcanogenic massive sulfides; evidence from sulfide mineralogy and the composition of sphalerite; Economic Geology and the Bulletin of the Society of Economic Geologists, v. 84, p. 1978–1995. doi:10.2113/gsecongeo.84.7.1978

Hannington, M.D., Poulsen, K.H., Thompson, J.F.H., and Sillitoe, R.H., 1999. Volcanogenic gold in the massive sulfide environment; Reviews in Economic Geology, v. 8, p. 325–356.

Lode, S., Piercey, S.J.P., Copeland, D.A., Devine, C.A., and Sparrow, B., 2012. Setting and styles of hydrothermal mudstones near the Lemarchant volcanogenic massive sulfide (VMS) deposit, Central Mobile Belt, Newfoundland; *in* Abstracts Volume 35, GAC-MAC Joint Annual Meeting, St. John's, Canada, May 27–29, 2012, 166 p.

McNicoll, V., Squires, G., Kerr, A., and Moore, P., 2010. The Duck Pond and Boundary Cu-Zn deposits, Newfoundland: new insights into the ages of host rocks and the timing of VHMS mineralization; Canadian Journal of Earth Sciences, v. 47, p. 1481–1506. doi:10.1139/E10-075

Piercey, S.J. and Hinchey, J.G., 2012. Volcanogenic massive sulphide (VMS) deposits of the Central Mobile Belt, Newfoundland, Geological Association of Canada–Mineralogical Association of Canada Joint Annual Meeting, Field Trip Guidebook B4. Open File NFLD/3173, Newfoundland and Labrador Department of Natural Resources, Geological Survey, 56 p.

Rogers, N., van Staal, C.R., McNicoll, V., Pollock, J., Zagorevski, A., and Whalen, J., 2006. Neoproterozoic and Cambrian arc magmatism along the eastern margin of the Victoria Lake Supergroup: A remnant of Ganderian basement in central Newfoundland; Precambrian Research, v. 147, p. 320–341. doi:10.1016/j.precamres.2006.01.025

Roth, T., Thompson, J.F.H., and Barrett, T.J., 1999. The precious metal-rich Eskay Creek Deposit, northwestern British Columbia; Reviews in Economic Geology, v. 8, p. 357–373.

Shimazaki, Y., 1974. Ore minerals of the Kuroko-type deposits; The Society of Mining Geologists of Japan, Special Issue, no. 6, p. 311–322.

Sillitoe, R.H., Hannington, M.D., and Thompson, J.F.H., 1996. High sulfidation deposits in the volcanogenic massive sulfide environment; Economic Geology and the Bulletin of the Society of Economic Geologists, v. 91, p. 204–212. doi:10.2113/gsecongeo.91.1.204

Squires, G. and Moore, P., 2004. Volcanogenic massive sulphide environments of the Tally Pool Volcanics and adjacent area; geological, lithogeochemical and geochronological results: Newfoundland Department of Mines and Energy, Geological Survey, Report 04-1, p. 63-91.

Squires, G.C.S., Brace, T.D., and Hussey, A.M., 2001. Newfoundland's polymetallic Duck Pond Deposit: earliest Iapetan VMS mineralization, formed within a sub-seafloor, carbonate-rich alteration system; *in* Geology and mineral deposits of the Northern Dunnage Zone, Newfoundland Appalachians, (ed.) D.T.W. Evans and A. Kerr; Geological Association of Canada – Mineralogical Association of Canada (GAC–MAC) Annual Meeting, St. John's, Nfld., 2001, Field Trip Guide A2, p. 167–187.

van Staal, C.R., Dewey, J.F., Niocaill, C.M., and McKerrow, W.S., 1998. The Cambrian-Silurian tectonic evolution of the northern Appalachians and British Caledonides: history of a complex, west and southwest Pacific-type segment of Iapetus; Geological Society of London, Special Publications, v. 143, p. 197–242. doi:10.1144/GSL.SP.1998.143.01.17

van Staal, C.R., Whalen, J.B., McNicoll, V.J., Pehrsson, S., Lissenberg, C.J., Zagorevski, A., van Breemen, O., and Jenner, G.A., 2007. The Notre Dame arc and the Taconic orogeny in Newfoundland; Geological Society of America, v. 200, p. 511–552. doi:10.1130/2007.1200(26)

White, J.D.L. and Houghton, B.F., 2006. Primary volcaniclastic rocks; Geology, v. 34, p. 677–680. doi:10.1130/G22346.1

Zagorevski, A., Van Staal, C.R., McNicoll, V., and Rogers, N., 2007. Upper Cambrian to Upper Ordovician peri-Gondwanan Island arc activity in the Victoria Lake Supergroup, Central Newfoundland: Tectonic development of the northern Ganderian margin; American Journal of Science, v. 307, p. 339–370. doi:10.2475/02.2007.02

Geological Survey of Canada Project 340321N461